Hydrogen adsorption and etching on the Si-rich 3C-SiC(001) 3×2 surface: First-principles molecular dynamics calculations

Peter Deák,[*] Bálint Aradi, Jan M. Knaup, and Thomas Frauenheim

Bremen Center for Computational Materials Science, University of Bremen, Am Fallturm 1, D-28359 Bremen, Germany
(Received 7 November 2008; revised manuscript received 21 January 2009; published 23 February 2009)

Atomic hydrogen adsorption on the silicon-rich 3C-SiC(001) 3×2 surface is investigated by means of first-principles molecular-dynamics calculations. Considering nearly fifty surface structures with 2–14 hydrogen atoms per unit cell, we show that up to a critical partial pressure of atomic hydrogen the equilibrium is represented by two or four hydrogen atoms adsorbed onto the two topmost Si atoms, causing complete passivation. These stable semiconducting structures are compatible with observations by scanning tunneling microscopy (STM) and core-level photoelectron spectroscopy (PES). Above the critical pressure, etching of the excess silicon sets in, but the etched surface is again semiconducting. Frequencies and infrared (IR) intensities of the vibration modes, calculated for the dihydrogenated surface, appear to be compatible with the observed IR spectrum, but none of the investigated metastable metallic structures is. It is also shown that the appearance of partially filled states near the Fermi level, as observed by PES and STM, can also be explained by a completely passivated surface, when taking into account the band bending effects due to surface dangling bonds and due to the spontaneous polarization before and after the hydrogenation, respectively.

I. INTRODUCTION

Interaction of hydrogen with a semiconductor surface often occurs in technological processes, such as chemical vapor deposition or dry etching. Well-controlled surface treatments with atomic hydrogen can also be used for nanostructuring. Hydrogen adsorption on the surface usually leads to chemical and electrical passivation but, curiously, upon exposure of the silicon-rich 3C-SiC(001) 3×2 surface to atomic hydrogen, the formation of one-dimensional metallic chains has been reported.[1–3] Exhaustive investigation of the arising hydrogenated surface by scanning tunneling microscopy (STM), scanning tunneling spectroscopy (STS), core-level spectroscopy [x-ray photoelectron spectroscopy (XPS)], and valence-band photoelectron spectroscopy [ultraviolet photoelectron spectroscopy (UPS)], as well as infrared-absorption spectroscopy (IRAS), have led to a detailed model of this surface, with four hydrogen atoms per surface unit cell and a row of Si dangling bonds. The latter was assumed to give rise to the metallic surface conduction [Fig. 1(a)].

Subsequent first-principles theoretical calculations on this model[4–7] equivocally showed that such a dangling-bond row does not exist (at 0K), and the metallicity stems from a row of Si-H-Si three-center bonds [Fig. 1(b)]. More detailed studies of the H adsorption[7,8] have shown that neither of the previous models represents the global energy minimum, which is, in fact, semiconducting [Fig. 1(c)]. It was argued, however, that kinetic factors favor a metastable metallic structure (not shown here), which is 1.6 eV higher in energy.[8] It should also be noted that, except for extremely low hydrogen partial pressures, a dihydride surface was predicted to be more stable than a monohydride one.[7] Figure 1(d) shows the most stable structure with four hydrogen atoms per surface unit cell, which is also semiconducting.

Based on the XPS (Ref. 9) and IRAS (Ref. 10) data, the results of the *ab initio* calculations have recently been challenged. Both papers conclude that the surface prepared at 300 °C, and investigated at room temperature, cannot be accounted for by static calculations at 0K, which fail to yield the model [Fig. 1(a)] considered by the authors as the only one compatible with all experimental data.

We have performed *ab initio* molecular-dynamics (MD) calculations at 300 °C, starting from the structure found in earlier calculations [Fig. 1(b)]. Instead of observing the appearance of the structure shown in Fig. 1(a), even a short anneal leads to a transformation of the silicon adlayers similar to the one shown in Fig. 1(c). This means that the original models, suggested by experiment [Fig. 1(a)] and by theory [Fig. 1(b)], have to be both discarded. Therefore, we carried out an extensive study of hydrogen absorption from two to 14 H atoms per surface unit cell. Since the observed metallicity seems to correlate with the appearance of a "hard" Si-H stretching mode in the IR spectrum at 2140 cm^{-1}, we have calculated the vibration frequencies and IR intensities for the most stable and for some of the metastable (metallic) structures at every H coverage. Our work is presented here as
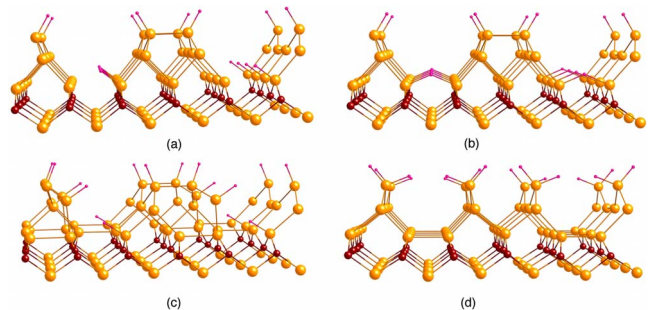

FIG. 1. (Color online) Various models of the 3C-SiC(001) 3×2 surface with four H atoms per surface unit cell (2×2 units are shown). For details, see the text. Large light (tangerine), medium dark (cayenne), and small dark (strawberry) spheres represent Si, C, and H atoms, respectively.
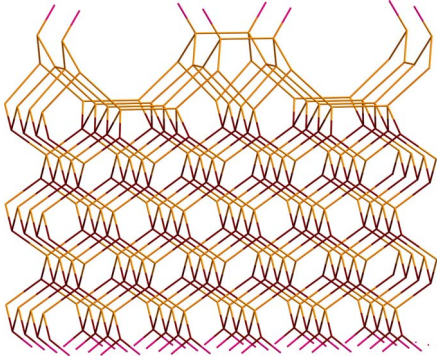
FIG. 2. (Color online) 2×2 units of the slab used for modeling the 3×2 reconstructed hydrogenated silicon-rich (001) surface of $3C$-SiC(001). The bonds are color-coded according to the connected atoms as described in Fig. 1. In our starting $T_1(200)$ structure the topmost Si dimers are monohydride passivated.

follows. Section II describes the applied methods. In Sec. III the investigated structures and their energetics are given, while Sec. IV deals with the vibrations. In Sec. V we discuss these results in light of the experimental STM, XPS, and IRAS data. Finally in Sec. VI we address the origin of the partially filled states, observed in STS and UPS.

II. METHODS

A slab model of the silicon-rich $3C$-SiC(001) 3×2 surface was used with five double layers (DLs) of SiC as substrate, saturated by H atoms on the C face, and with 15 Å of vacuum above the topmost silicon adlayer. Calculations have been performed on the 3×2 reconstructed surface unit cell, with a 2×3 Monkhorst-Pack sampling[11] of the Brillouin zone. Figure 2 shows 2×2 units of the monohydride covered supercell, which contains three silicon layers in the upper part: from top 1/3, 2/3, and 1 monolayer (ML). The Si atoms form dimers in all three layers. The equilibrium structure has been obtained after fixing the atoms of the bottom DL in positions obtained in a bulk calculation. (In subsequent geometry optimizations with further hydrogen adsorption, the terminating H atoms on the backside have also been kept fixed.) The dimers all are symmetric when the topmost dimer is hydrogen saturated. In the following, we will denote this silicon backbone as T_1. (In Fig. 3 of Sec. III, we will introduce two other structures for the Si adlayers.) For the hydrogenated surface we will use the notation $T_i(lmn)$, where the integers in the parentheses denote the number of H atoms attached to the Si atoms in the topmost, middle, and lowest silicon layer, respectively. [Fig. 2 shows the $T_1(200)$ structure.]

Calculations have been carried out in the local (spin) density approximation (LDA) using the Vienna *ab initio* simulation package (VASP) 4.6, with the projector augmented wave method.[12] The plane-wave cutoff was set to 420 eV for the wave-function expansion, and to 840 eV for that of the charge density. The equilibrium structures have been determined using the convergence criteria of 1×10^{-4} eV and 0.01 eV/Å^2 for the electronic and ionic degrees of freedom

and a grid for fast Fourier transformation (FFT) determined by 1.5 times the wave-number cutoff. Based on chemical intuition and experience with interstitial H in Si and SiC,[13,14] about 50 different surface structures with 2–14 hydrogen atoms per surface unit cell have been considered. Conjugate gradient relaxation at 0K was followed, in case of the most stable structures at each H coverage, by MD anneals at 300 °C for 500–2000 fs (after a 500 fs ramp), in steps of 2 fs, to check on the temperature stability of the 0K structures. The most stable structures have been reoptimized with the generalized gradient approximation (GGA) using the PW91 functional.[15] Then convergent surface phonon frequencies have been calculated in the harmonic approximation at the Γ point, allowing only the Si-H units to move, but tightening the convergence criteria for electronic and ionic relaxation to 1×10^{-5} eV and 0.005 eV/Å^2, respectively, and using twice the wave-number cutoff to determine the grid for FFT. Regarding the difficulties in calculating convergent IR intensities with a plane-wave basis set, for that purpose the density-functional-based tight-binding (DFTB) method was utilized on a valence Slater basis set.[16] The equilibrium DFTB geometry was sufficiently close to the *ab initio* one.

The relative stability of the various structures have been compared as a function of the chemical potential of atomic hydrogen in the gas phase, as described by Peng *et al.*[7] [with the zero point energy (ZPE) of Si-H stretching vibrations included in the total energy]. As reference point, however, the experimental (-1 Ry) rather than the LDA energy (-0.89 Ry) of atomic hydrogen was used since the experimental dissociation energy of the H$_2$ molecule is much better reproduced this way. For the LDA electronic structure calculations we applied a thicker slab, consisting of nine SiC double layers, saturated with H on the C face, and with 21 Å of vacuum between the slabs.

III. ENERGETICS OF HYDROGEN ABSORPTION

It has already been mentioned in Sec. I that a relatively short MD on the metallic $T_1(202)$ structure resulted in a
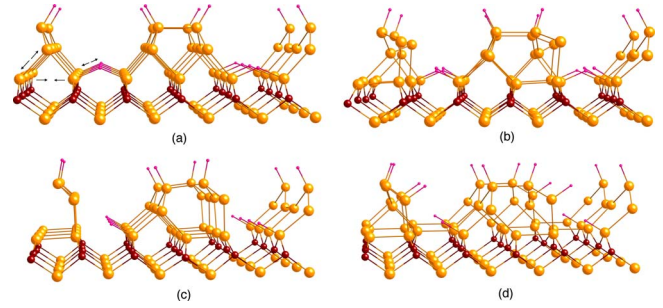

FIG. 3. (Color online) Transformation of the metallic $T_1(202)$ structure (a) into the more stable semiconducting Mix(202) structure (b) which is—as far as the Si backbone is concerned—a mixture of the (a) T_1 and (c) T_2 reconstructions of the Si layers. The arrows in (a) show the bond breaking and formation leading to (c). The metallic $T_2(202)$ structure (c) is the least, while the semiconducting Mix(211) structure (d) the most stable one with four H atoms per cell and monohydride saturation of the surface dimer.

transformation of the Si adlayers. As shown in Fig. 3, the Si-H-Si bridge breaks indeed, but a Si-Si bond between atoms of the lowest and the middle silicon layer breaks as well, while a dimer bond is formed in the third silicon layer. If that happened to both Si-H-Si bridge in the unit cell, one would arrive at the structure termed $T_2(202)$ in Fig. 3(c), with a dangling-bond row on the Si atoms in the middle layer. This metallic structure is, however, less stable than the starting $T_1(202)$. In fact, the MD ends up with the Mix(202) structure [Fig. 3(b)], where half the unit cell has a T_1, the other half a T_2 reconstruction, with one middle-layer dangling bond and one lowest-layer Si-H-Si bridge per cell. The states corresponding to the latter lie higher in energy than those of the former. Therefore the band of Si-H-Si states is empty, while that of the dangling bonds is doubly occupied. Therefore, the Mix(202) structure is semiconducting. It is 0.14 eV lower in energy than the metallic $T_1(202)$ structure. A nudged elastic band calculation of the transformation barrier gives 0.48 eV. If the hydrogen atom is taken out of the Si-H-Si bridge and the dangling bond on the middle-layer Si atoms is saturated instead, one arrives at the semiconducting structure of Peng *et al.*[8] [Fig. 3(d)] with an energy gain of 1.19 eV.

Peng *et al.*[8] showed that the Mix(211) structure is more likely to form spontaneously than the $T_1(202)$. Here we see that even if one starts with $T_2(202)$, the Si backbone would transform at 300 °C anyhow. Therefore, based on the energetics, the $T_1(202)$ structure (both with Si-H-Si or with Si····H-Si configuration) must be excluded. Table I shows the formation energies of the most stable surface structures with respect to the hydrogen free $3C$-SiC(001) 3×2 surface and free hydrogen atoms (at 0K). The structures with the lowest energy at each coverage are depicted in Fig. 4. As can be seen, at least six hydrogen atoms per unit cell are needed to stabilize the T_2 adlayer reconstruction. For monohydride saturation of the top dimers and with less than six hydrogen atoms per unit cell, the mixed reconstruction is the most stable, except for the starting $T_1(200)$ structure. However, as already found by Peng *et al.*,[7] the dihydride saturation is favored, and the $T_1(400)$ structure has the lowest formation energy per H atom for systems with more than two hydrogen atoms per unit cell.

A general feature is that the formation energy per H atom for systems with an odd number of hydrogen is higher than the most stable ones with one H more or less. Obviously, dangling bonds are not favorable if atomic H is present. In systems with even number of H atoms the ground state is always semiconducting. With 12 H atom per unit cell in the system, the lowest energy is achieved when $(Si_3H_6)_n$ chains dissociate from the surface. The polymer is probably an artifact of the confined space and symmetry of the slab model, but it indicates that oligosilanes are likely to dissociate around this coverage, i.e., the etching of the Si adlayers begins.

The evolution of the surface structure upon increasing the atomic hydrogen concentration can be followed by depicting the formation energy as a function of the chemical potential of atomic hydrogen—which is, at constant temperature, a monotonic function of the partial pressure. This is shown in Fig. 5.

TABLE I. Formation energy, E_f, of the most stable structures with respect to the clean surface and atomic hydrogen at 0K. N is the number of H atoms in the system.

N	Structure	E_f (eV)	E_f/N (eV)	Nature
2	$T_1(200)$	−5.78	−2.890	Semiconducting
3	Mix(210)	−6.10	−2.034	Metallic
3	Mix(201)	−6.16	−2.054	Metallic
3	$T_1(300)$	−6.23	−2.078	Metallic
4	$T_2(220)$	−6.63	−1.658	Metallic
4	$T_2(202)$	−7.30	−1.824	Metallic
4	$T_1(202)$	−7.69	−1.923	Metallic
4	Mix(202)	−7.83	−1.957	Semiconducting
4	Mix(211)	−9.01	−2.253	Semiconducting
4	$T_1(400)$	−9.39	−2.348	Semiconducting
5	Mix(212)	−9.95	−1.990	Metallic
6	$T_1(222)$	−9.12	−1.520	Metallic
6	$T_1(204)$	−10.43	−1.739	Semiconducting
6	$T_1(402)$	−10.82	−1.803	Metallic
6	$T_2(402)$	−10.82	−1.803	Semiconducting
6	$T_2(222)$	−12.56	−2.093	Semiconducting
7	$T_2(322)$	−12.92	−1.846	Metallic
8	$T_1(422)$	−12.38	−1.548	Metallic
8	$T_1(440)$	−13.95	−1.744	Semiconducting
8	$T_2(224)$	−13.98	−1.747	Metallic
8	$T_2(242)$	−14.04	−1.755	Metallic
8	$T_2(422)$	−16.00	−1.999	Semiconducting
9	$T_2(342)$	−15.54	−1.727	Metallic
10	$T_2(442)$	−17.45	−1.745	Metallic
10	$T_2(244)$	−18.30	−1.830	Semiconducting
11	$T_2(452)$	−20.12	−1.829	Metallic
12	$T_2(264)$	−20.13	−1.678	Metallic
12	$T_2(462)$	−21.60	−1.800	Semiconducting
12	$T_2(444)$	−22.11	−1.843	Semiconducting
12	Dis(204)+$(Si_3H_6)_n$	−22.72	−1.893	Semiconducting
14	$T_2(464)$	−23.77	−1.698	Metallic
14	$T_2(464)$	−24.26	−1.733	Semiconducting

As can be seen, the two most stable metallic systems are not even near of being the equilibrium at any atomic hydrogen pressure. In the low-pressure range this is the semiconducting $T_1(400)$ structure [Fig. 1(d)] with a simple dihydride saturation of the topmost Si dimer. [$T_1(200)$ is the equilibrium only for H pressures near to the vacuum background pressure in the chamber (see vertical line in Fig. 5.)] The $T_1(400)$ structure arises spontaneously from The $T_1(300)$ structure upon addition of another hydrogen. Since the latter
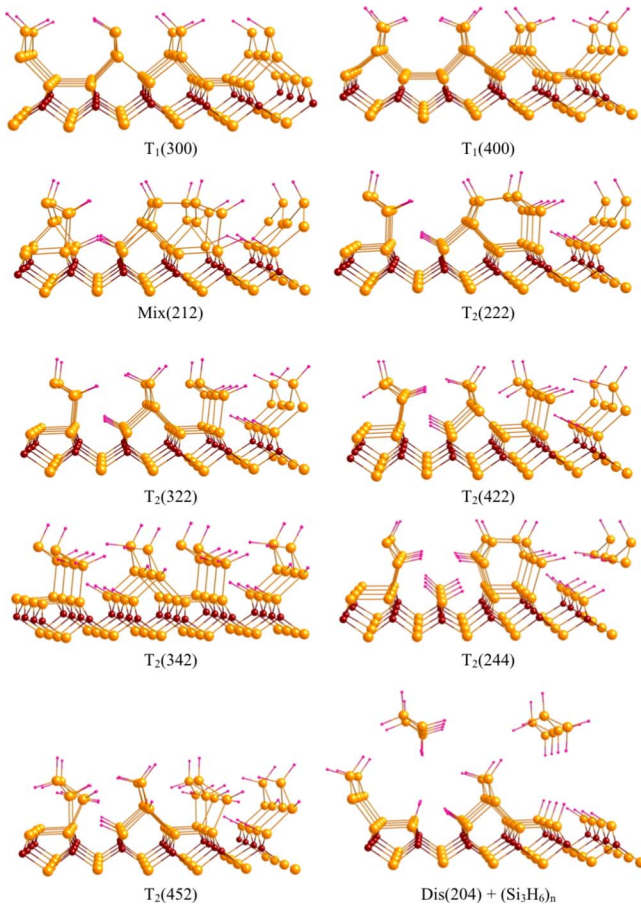
FIG. 5. (Color online) Formation energies as a function of the chemical potential of atomic hydrogen, μ_H. (The zero point of the scale is chosen at the energy of the H atom at 0K.) The vertical line marks the μ_H value corresponding to 1×10^{-10} Torr atomic hydrogen pressure at 300 °C. (For constant temperature, increasing μ_H values correspond to increasing pressure.) The most stable metallic structures are shown with thin solid (red) lines. Dashed (blue) lines show semiconducting structures of high stability. The thick (black) lines correspond to the equilibrium structures in the low- and high-pressure range.

FIG. 4. (Color online) The most stable structures at each H coverage between three and 12.

forms also spontaneously from the $T_1(200)$ monohydride surface, the $T_1(400)$ structure must be dominant up to the atomic hydrogen pressure where etching sets in. After removal of three Si atoms per unit cell (Fig. 4 bottom right), the equilibrium structure is again semiconducting. (This is true even after further hydrogenation of the etched surface.) The unetched surface with more than 12 H atoms is not the equilibrium for any reasonable atomic H concentration.

IV. VIBRATIONS

A crucial point of the observations on the hydrogenated $3C$-SiC(001) 3×2 surface is a 2140 cm^{-1} Si-H stretching mode, appearing simultaneously when free-carrier absorption is also observed.[2,10] This peak appears also if the hydrogenation was carried out after water absorption and survives oxidation. In case of pure hydrogenation, an additional spectral feature with a peak at 2118 cm^{-1} and a shoulder around 2110 cm^{-1} has been assigned to monohydride saturation of the topmost dimers, while a broad peak, appearing at 2100 cm^{-1} in both s- and p-polarized light, was attributed to the Si-H bonds on the backside of the silicon holder used in the multiple back-reflection measurement.

The accurate calculation of IR frequencies is a very difficult task. While we have taken great care of obtaining convergent values (k-point set and coupling to vibrations of the
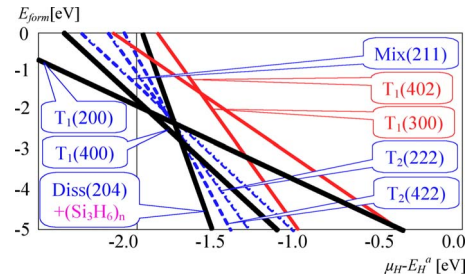
neighbor Si layers have also been checked), the source of greatest error still remains. The Si-H stretching vibrations are strongly anharmonic, and the harmonic approximation may lead up to 5% overestimation of the observed values. The anharmonicity is influenced by the electrostatic interaction of nearby hydrogen atoms (as in the hydrogenated vacancy in bulk Si or as in the SiH$_4$ molecule), but is inherent to a single and relatively well-isolated Si-H bond as well. We have performed reference calculations for the hydrogenated Si(111) 1×1, $3C$-SiC(111) 1×1, and Si(001) 3×1 surface. The former two contain only monohydrides far from each other for significant electrostatic interactions. The latter has an alternating dihydride and monohydride saturation, where the H atoms of a dihydride and a monohydride are relatively close. The calculated results are compared to experimental data[17–19] in Fig. 6.

As can be seen, the values scatter around a straight line within ~10 cm^{-1} due to the hydrogen-hydrogen interactions. To screen out systematic errors, including the anhar-

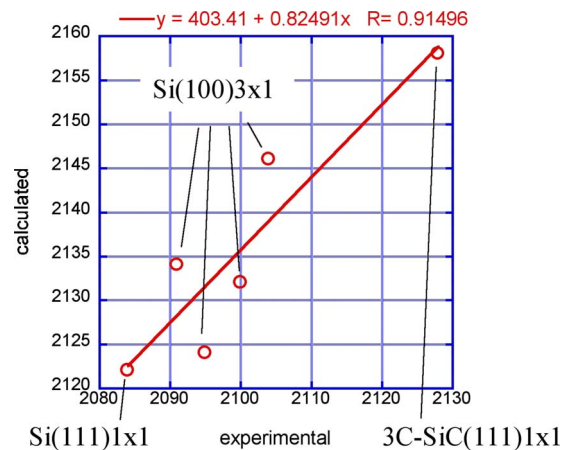FIG. 6. (Color online) Correlation between the calculated and measured Si-H stretching frequencies for three known hydrogenated surfaces. The thick line was obtained in a RMS fit, as shown above the diagram. For details see text.

TABLE II. Si-H stretching modes of the $T_1(400)$ surface. The arrows indicate the relative motion of the hydrogen atoms [cf. Fig. 1(d)].

Mode	Calc. frequency (cm^{-1})	Calc. relative intensity
↖ ↙ ↘ ↗	2151	1.0
↖ ↙ ↘ ↙	2134	17.6
↖ ↗ ↘ ↙	2115	5.5
↖ ↗ ↖ ↗	2110	0.9

monicity of a single isolated Si-H bond, we use the straight line, obtained by an rms fit, as a calibration curve when comparing the frequencies calculated for the $3C$-SiC(001) 3×2 surface with experiment. Table II shows the stretching modes of the dihydride saturated $T_1(400)$ surface. The resulting values are well within the range of the observed ones of 2140, 2118, and 2110 cm^{-1}, but are somewhat higher, which can be explained by the decoupling from the rest of the phonon spectrum and the Γ approximation on the theoretical side, and by the known difference between frequencies measured at room temperature and in fluid helium. It is interesting to note that the calculated relative intensities of the three higher modes follow the measured ones[2] rather well, while the weak lowest one could have been masked by the broad backside Si-H band at 2100 cm^{-1}.

Using the same approximations we have also calculated the Si-H vibrations for many of the structures given in Table I. The structures containing more than four H atoms show a multitude of IR active stretching modes, which apparently do not show up in the experimental spectrum. The stretching modes of the most stable metallic systems are 2106, 2072, and 2045 cm^{-1} for $T_1(300)$, and 2166, 2149, 2103, 2097, 1329, and 1291 cm^{-1} for $T_1(402)$. Obviously, neither of them can explain the observed vibrations. (Note that the calibration curve is invalid for the tri-center Si-H-Si bond in this structure so the real frequencies of the lowest two modes are probably closer to 1400 cm^{-1}.) For the two higher modes of the $T_1(202)$ structure we have obtained 2104 and 2098 cm^{-1} (and a low-lying mode around 1400 cm^{-1}), in agreement with others. The Mix(211) structure results in modes at 2098, 2080, 2013, and 1975 cm^{-1}. From all the structures we have considered, only the $T_1(400)$ has vibration frequencies in number and value close to the observed ones. It is interesting to note, that a Si-H bond in the vicinity of a dangling bond always yields a low-frequency vibration. For example, Fig. 7 shows a metastable metallic structure on the etched surface, E(202). The stretching mode of the Si-H bond near the dangling bond has a frequency around 1550 cm^{-1}. Therefore, even if the structure suggested in Fig. 1(a) existed, it could not explain the hard Si-H stretching mode.
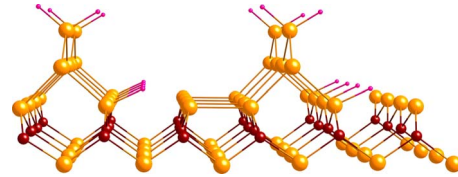

FIG. 7. (Color online) The metastable metallic E(202) structure which may arise after etching, and contains Si-H bonds near to dangling bonds. The resulting stretch mode is around 1550 cm^{-1}. For details, see text.

V. DISCUSSION OF THE EXPERIMENTAL STM, XPS, AND IRAS RESULTS

The model in Fig. 1(a) was suggested to explain the following experimental observations:[1,9,10] (i) band-gap closing in the I/V characteristics by STS, (ii) buildup of states at the Fermi level by UPS, (iii) three spectral features at 2140, 2118, and 2110 cm^{-1} in IRAS, the first one appearing simultaneously with free-carrier absorption between states near the Fermi level, (iv) symmetric position of the Si atoms in the topmost layer by STM, and (v) appearance of a fourth surface-related component with respect to the bare surface in the XPS spectrum. Even if this model was not unfavorable energetically, its value for explaining these observations could be questioned. Although it would definitely be metallic, in line with the STS observation, the band of singly-occupied dangling bonds would be in the middle of the band gap (cf. the positions of the doubly-occupied and empty dangling-bond bands of the bare surface in Sec. VI), which is incompatible with the UPS data. The hydrogenation makes the topmost Si dimer symmetric, in accord with the STM picture, but at the same time makes any assignment of the four surface-related XPS components to the features observed on the bare surface obsolete. The chemical shift (CS), observed in XPS, is primarily determined by the charge state of the atom and by the nearest neighbors. As it was shown theoretically,[20] the five inequivalent Si atoms of the bare surface should lead to CS (with respect to the SiC bulk) as follows: the down (formal charge +1) and the up atoms (formal charge −1) of the topmost dimer: +0.08 and −0.65 eV, respectively, the atoms of the middle-layer dimer, connected to the down and to the top atoms of the upper layer: −0.28 and −0.56 eV, respectively, and, finally, atoms in the third layer: −0.3 eV. (Due to the 0.08 eV spectral resolution, only three components are observed in XPS.[9]) Obviously, the two different CS caused by the up and down atoms will be replaced by a single one of the hydrogenated symmetric dimer, which is unrelated in energy to any of the formers. The two different shifts of the dimers in the middle layer will also collapse into one in a similar manner. Therefore, the only hard fact is that four different CS are observed on the hydrogenated surface, and any model should have at least four inequivalent Si atoms in the three silicon adlayers. The one in Fig. 1(a) has *five*: atoms of the hydrogenated topmost dimer, atoms of the dimers in the middle layer, as well as three different Si atoms in the third layer—one with two Si, one with one Si and one H, and one with one Si neighbor and a dangling bond (besides the two C neighbors for all). It is

conceivable that one of these five CS cannot be resolved, but the XPS result cannot be used to support the specific model of Fig. 1(a) directly. The same is true for the IRAS results. As shown in Sec. IV, a Si-H bond next to a dangling bond has a very low stretching mode frequency, and cannot account for the peak at 2140 cm^{-1}. We also note that, due to the low symmetry of the model in Fig. 1(a), the vibrations of the two H atoms attached to the third layer Si atoms are not degenerate. The coupling between them is, however, strong, causing a splitting of the stretching frequency, which should be observable in IRAS. (For the system shown in Fig. 7 we calculate a splitting of 35 cm^{-1}.) Finally, our MD studies refute the expectation that increasing temperature will stabilize the Si$\cdots$H-Si configuration of Fig. 1(a) over the Si-H-Si bridge of Fig. 1(b). This is actually not too surprising. The three-center bond of hydrogen in semiconductors is a regular phenomenon under certain circumstances,[21] and occurs even at room temperature in bulk silicon.[13] The surprise is that the T_1 structure of the Si layers is not stable at 300 °C over three H atoms per surface unit cell and monohydride passivation of the topmost layer. We believe, therefore, that both models shown in Figs. 1(a) and 1(b) must be discarded.

From the energetics alone, all monohydride saturated T_1-type structure could be rejected, except for the $T_1(200)$ structure at very low concentration of atomic hydrogen in the gas phase. [We note that the metastable $T_1(220)$ structure suggested by Peng *et al.*[8] has a low- but no high-frequency mode, and contains only three differently coordinated Si atoms, and is, therefore, incompatible with the IRAS and XPS data as well.] The Mix and T_2 structures are more stable than the T_1 ones in case of monohydride saturation, but they seem to be incompatible with the STM picture due to the asymmetric position of the atoms in the top most Si dimers. In fact, however, as shown in Fig. 5, the dihydride saturated $T_1(400)$ structure is the most stable one in the low hydrogen pressure range.

The dihydride saturation has been rejected for two reasons,[9,10] based on experience with hydrogenated silicon surfaces: the preparation temperature is lower than the one necessary for achieving the dihydride surface in silicon, and the peak at 2140 cm^{-1} is higher than the stretching modes observed on that surface. Regarding the first argument we note that the troughs between the top dimers of the 3*C*-SiC(001) 3×2 reconstruction will lead to much smaller steric repulsion energies upon hydrogenation of the top dimers than in the case of the Si(001) surface, and the Si-Si bonds are probably also somewhat weaker due to charge transfer to the C atoms in the SiC substrate. Therefore, dihydride formation can occur at lower temperatures even in a H$_2$ atmosphere. Atomic hydrogen is known to attack the Si-Si bonds aggressively even in bulk silicon, so it is no surprise that we find the spontaneous formation of $T_1(400)$ in their presence. As for the 2140 cm^{-1} mode, it was argued that such a high frequency can only be expected from a C-Si-H configuration, for the frequency of the Si-H bond was found to be 2128.4 cm^{-1} on the hydrogenated 3*C*-SiC(111) surface.[18]

Concerning trends in Si-H stretching frequencies, two factors must be considered. One is the number of H atoms bonded to the same Si atom; the other is the electronegativity

TABLE III. Experimentally observed frequencies (in cm^{-1}) of Si-H stretching mode vibrations in molecules and on surfaces (left two columns) and in the bulk vacancy of silicon (right two columns). For references see Ref. 23. "Me" stands for methyl groups. For surfaces the orientation and surface cell size is indicated.

(Me)$_2$SiH$_2$	2165, 2143	Si:V(4H)	2210
Cyclo-(SiH$_2$)$_6$	2128, 2120	Si:V(3H)	2162
3*C*-SiC(111)H 1×1	2128	Si:V(2H)	2066
(Me)$_3$SiH	2118	Si:V (H)	2055
Si(111)H 1×1	2084		

sum of the other neighbors.[22] Increasing either of the two, the Si-H stretching frequency increases as well. Table III shows a compilation of data for Si-H bonds in a predominantly vacuum environment and in bulk silicon. The latter shows that the steric repulsion of nearby Si-H bonds increases the frequency even more. Based on the trends observed also in Table III, a Si-H bond with only two C neighbors should have a lower frequency than the 2128.4 cm^{-1} mode observed on 3*C*-SiC(111), where the Si-H bond has three. A higher frequency can only be expected either for a dihydride with two carbon neighbors or if nearby Si-H bonds are present. The latter is, however, also true for a dihydride with only silicon neighbors. This is the situation for the $T_1(400)$ structure, resulting in a high-frequency mode, indeed [cf. the lower frequencies of the $T_1(300)$ structure].

As for other structures: a higher number of hydrogen atoms leads to a higher number of IR modes, which are not observed. This is also consistent with the message of Fig. 5: for higher atomic hydrogen concentration etching of the Si adstructure begins. This prediction is perfectly in line with the known fact that atomic hydrogen etches silicon (see, e.g., the dry etching performed by an atomic hydrogen beam) because atomic hydrogen attacks the Si-Si bonds (cf. the SmartCut® process).

Regarding the energetics and the vibrations, only the $T_1(400)$ structure seems to be realistic for the hydrogenated 3*C*-SiC(001) 3×2 surface. It also complies with the observed STM image, at least where the repetition of two equally bright spots are concerned, due to the symmetric position of the SiH$_2$ units. (No STM image simulation has been performed though.) It should also be noted that the $T_1(400)$ structure contains exactly four inequivalent silicon positions: one in each of the top and middle layer, and two in the third one [Fig. 1(d)]. The latter two both have two Si and two C neighbors, but the two Si atoms in the third layer dimer may be differently affected by the charge transfer due to hydrogenation than the one between two dimers. It seems likely that this shows up in the small difference between the "R" and "S3" component of the XPS spectrum,[9] mirroring also the 1:2 ratio of atoms in these two inequivalent positions.

Finally, we would like to comment on the observations that (i) the mode around 2140 cm^{-1} shows up also in samples hydrogenated after water dissociation on the bare surface, and (ii) it persists when the hydrogenated surface is oxidized.[2,10] In case (i), it was assumed[2,10] that hydrogena-
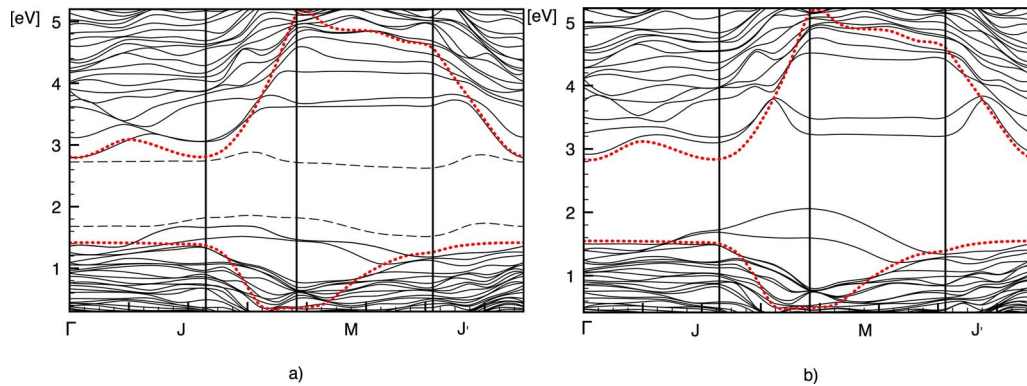
FIG. 8. (Color online) Band structures of the clean and the dihydrogenated 3C-SiC 3×2 (001) surface. The dotted lines are the projections of the bulk band edges of 3C-SiC onto the surface Brillouin zone. [The bands of the bulk and the slab calculations have been aligned by correcting for the shift of the average electrostatic potential at a bulklike atom (Ref. 24).] Dashed lines show the dangling-bond bands of the clean surface.

tion has moved the oxygen atom of the OH group—adsorbed on one of the Si atoms of the top dimer after water exposure—into this dimer bond, although no characteristic Si-O-Si mode was presented, and the Si-H mode shifted only 4 cm^{-1} with respect to the case where hydrogenation was carried out without previous water absorption. Based on the electronegativity sum rule,[22] such a scenario should have caused a much larger shift. According to our calculation, the H-Si-O-Si-H termination is, indeed, lower in energy than the H-Si-Si-OH one by 0.9 eV, but the Si-H modes calculated for the T$_1$(200) surface shift, on average, by ~13 cm^{-1}. When the oxygen atom is inserted into the third layer Si dimer, instead of that in the top layer, the energy gain is slightly less (0.8 eV) but the shifts are closer to the observed one: on average 6 cm^{-1}. It is, also, conceivable that atomic hydrogen simply replaces the OH groups on the surface, with the simultaneous formation of water. Indeed, we calculate an energy gain of −6.3 eV for the reaction H-Si-Si-OH+2H →H-Si-Si-H+H$_2$O. Hydrogenation would then proceed just as without preceding water absorption, only it created a less well-defined and less homogeneous surface, causing the observed small shift. In case (ii) no shift at all was observed upon oxidation in any of the three modes of the hydrogenated surface (2140, 2118, and 2110 cm^{-1}), while Auger spectroscopy has shown 1/3 ML oxygen insertion. It was suggested that oxygen attacks Si-Si bonds between the middle and the lowest layer of the adstructure.[2,10] As our result above indicates, even oxygen insertion into the Si adstructure furthest away from the top layer should cause a noticeable shift. In any event, the observed zero shift contradicts any model with oxygen being in the vicinity of the Si-H bonds.

VI. ELECTRONIC STRUCTURE

With all that said, the most interesting observations—the band-gap closing seen in STS, and the buildup of states at the Fermi level, as seen in UPS—seem not to be compatible with the semiconducting T$_1$(400) structure, which represents the equilibrium of the 3C-SiC(001) 3×2 surface at 300 °C up to atomic hydrogen concentrations where etching starts.

These observations suggest the presence of a partially filled band very near to the CB edge, while there are no obvious defect-related gap states in the T$_1$(400) structure. It could be possible that the metallicity stems from one of the metastable structures, but the correlation of the 2140 cm^{-1} band with the observation of free-carrier absorption makes that unlikely. At this point, it should be mentioned that all experiments but one UPS investigation have been carried out on n-type samples. The results presented in Table I (as those of all earlier calculations) relate to intrinsic samples. It is known that in n-type bulk silicon hydrogen prefers the so-called antibonding site (behind a Si-Si bond), and is negatively charged.[13] We have checked structures with hydrogen atoms antibonding to the Si atoms in the second layer, as well as in H$_2^*$-like pair configurations,[23] in the negative charge state—but for any position of the Fermi level these were less stable than the structures shown in Fig. 4. This is in line with the claim[1] that the structure of the hydrogenated surface does not depend on the nature of doping.

However, the doping concentration of the experimentally investigated[1–3,9,10] n-type samples were 5×10^{18} cm^{-3}, therefore, at room temperature they were conducting. The reason why that was not observed on the surface by STS must have been the band bending induced by the dangling-bond states on the surface.[1] Figure 8 shows the calculated band structure in the surface Brillouin zone for both the clean and the dihydride passivated surfaces (for a slab of 9 SiC DL in thickness). As it was noted earlier,[7,25,26] there are two dangling-bond bands in the gap of the clean surface. The lower one, related to the "up" atom in the asymmetric top layer Si dimers, is doubly occupied; the other, related to the "down" atoms, is empty. These states will act as surface traps for carriers in doped samples. The empty dangling-bond state at the Γ point is shown in Fig. 9(a). In n-type samples, the empty dangling bonds will pin the Fermi level by trapping electrons, and cause an upward band bending, which depletes the surface layer of free carriers. Indeed, UPS has indicated a 0.5 eV upward bending in these samples, with no occupied states near the Fermi energy, and a "gap" in STS.[1] To demonstrate this band bending, we simulated n-type doping by adding −0.1e charge to the system, corresponding to
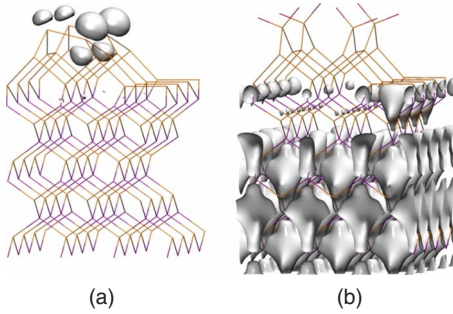
FIG. 9. (Color online) Square of the wave function for the lowest unoccupied state at Γ on the (a) clean and (b) dihydrogenated neutral surface. (1×2 unit cells of the 3×2 reconstructed surface are shown.)

an excess electron concentration of $\sim 1 \times 10^{20}$ cm^{-3} in our slab. The resulting electrostatic potential, averaged in planes parallel to the surface, and for double layers along the axis[27] is shown in Fig. 10(a). As can be seen (solid line), the potential in the SiC part rises indeed toward the Si face, where the charge is captured.

Hydrogen passivation, of course, means the removal of the dangling-bond states, as can be seen in Fig. 8(b). While the Si-Si bonds still give rise to occupied surface states near the VB edge, they create only resonances in the CB. The bottom of the CB follows the dispersion of the bulk curve, indicating that the states there are essentially bulklike. Figure 9(b) shows the one at the Γ point. Although infinite bulk $3C$-SiC has no spontaneous polarization, a finite slab has, leading to a slope in the average potential from the C face to the Si face.[28] This can clearly be seen in Fig. 10 (dashed lines) for both the clean and the hydrogenated surfaces in the neutral state. (We note that hydrogenation also creates a surface dipole layer due to the charge transfer from Si to H, but the arising potential shift in the slab scales with the Si-H distance, while that of the spontaneous polarization scales with the thickness of the slab. So the effect of the dipole layer is negligible with respect to the polarization field in a macroscopic slab.) In reality, the spontaneous polarization

field is compensated in the case of doping by the redistribution of the mobile carriers.[28] In our model calculation for the hydrogenated slab, although the extra charge is not trapped at the surface, the relatively small width of the slab does not provide a sufficient amount of mobile carriers, even with a concentration of $\sim 1 \times 10^{20}$ cm^{-3}. Therefore, the compensation is only partial [cf. the slopes of the solid and dashed curves in Fig. 10(b)]. It demonstrates, however, that if the excess electrons are not trapped in surface states (as was the case for the clean surface), the distribution of the mobile electrons will show an accumulation at the Si face to compensate the inherent polarization field.

Since the hydrogen passivation restores flat band conditions, and in *n*-type samples mobile electrons will accumulate at the surface, STS and UPS will show "band-gap closing" and the appearance of occupied states at the bottom of the CB, respectively. In fact, it is the partially filled conduction band which is now observed. Indeed, the energy difference to the VB edge was found to coincide with the band gap.[1] The UPS investigation of a *p*-type sample (doping level not known) has shown occupied states near the CB as well.[2] In *p*-type hydrogenated samples, the surface states near the VB [see Fig. 8(b)] would still capture holes, causing downward bending [see dash-dotted line in Fig. 10(b)] in the surface potential, and so depletion of the surface of free holes. At the same time, however, the minority carriers will accumulate. Since the *n*-type background of the investigated sample was quite high,[29] we believe that the accumulation of the minority carriers at the surface can explain the UPS observation on the *p*-type sample. One should also consider that UPS excites electrons into the CB, and those will also move toward the surface in case of downward band bending.

Therefore, due to the accumulation of mobile electrons at the surface, no half-filled defect band is needed to explain the STS and UPS results, and the fully passivated $T_1(400)$ structure is in no contradiction with them. [We note, that the argumentation above is also valid for the $T_1(200)$ structure, which is prevalent at very low atomic hydrogen exposures.]
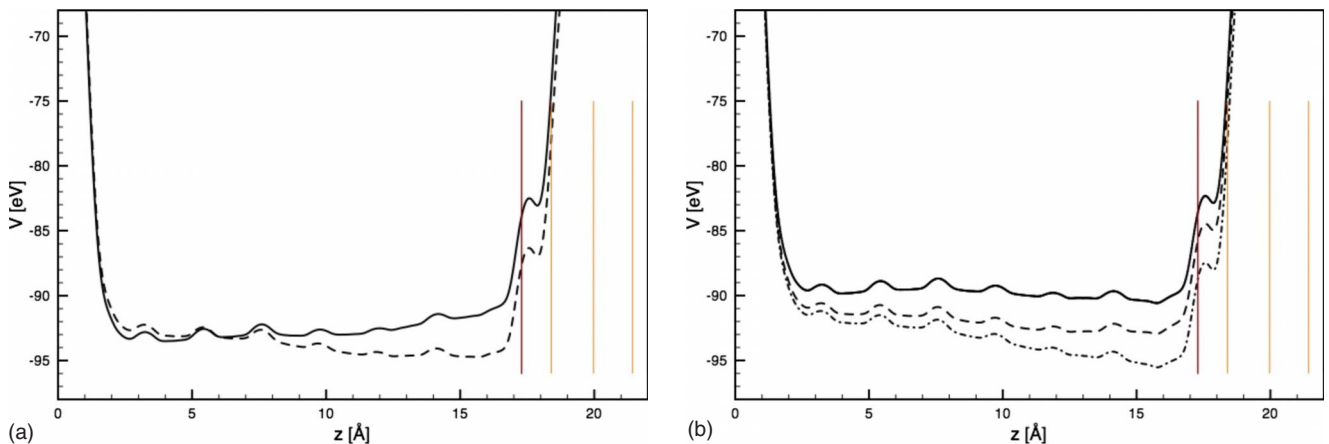

FIG. 10. (Color online) Average electrostatic potential along the slab axes for the (a) clean and the (b) hydrogenated surface. Solid lines refer to the negative, dashed ones to the neutral, and the dash-dotted one to the positive charge state. The dark vertical line marks the position of the uppermost carbon, the light ones the silicon adlayers for the hydrogenated surface.

VII. SUMMARY

In summary, meticulous static and MD calculations rule out the exotic dangling-bond row or even the Si-H-Si bridge row model for the hydrogenated $3C$-SiC(001) 3×2 surface, and establish a more prosaic dihydride saturation of the surface dimer as the equilibrium structure up to atomic hydrogen concentrations where etching starts. Our results are in agreement with the static calculations of Peng *et al.*,[7] and in line with the known energetics of Si-H bonds: atomic hydrogen first saturates the dangling bonds, then attacks Si-Si bonds, forming first a Si-H-Si bridge, then two Si-H bonds (for which the sum of binding energies is higher than that of a single Si-Si bond).[30] These trends lead to the etching of the Si adlayers as the H concentration increases. The dihydride saturated $T_1(400)$ structure is compatible with the STM and XPS observations, and—taking into account the accuracy of theory and the disturbing strong back-surface modes in experiment—the calculated vibration frequencies and intensities are consistent with the IRAS results. The "metallic" behavior of the surface, i.e., the appearance of partially filled states around the Fermi level, as observed by STS and UPS, respectively, *in doped samples*, can fully be explained taking into account the band bending effects before and after hydrogenation due to surface dangling bonds and the spontaneous polarization of SiC, respectively. The predictions of our calculations could be checked by scanning tunneling vibration spectroscopy[31] using also isotopes for hydrogenation.[32]

*deak@bccms.uni-bremen.de

[1] V. Derycke, P. G. Soukiassian, F. Amy, Y. J. Chabal, M. D'Angelo, H. B. Enriquez, and M. G. Silly, Nat. Mater. **2**, 253 (2003).

[2] F. Amy and Y. J. Chabal, J. Chem. Phys. **119**, 6201 (2003).

[3] P. G. Soukiassian and H. B. Enriquez, J. Phys.: Condens. Matter **16**, S1611 (2004).

[4] R. Di Felice, C. M. Bertoni, C. A. Pignedoli, and A. Catellani, Phys. Rev. Lett. **94**, 116103 (2005).

[5] H. Chang, J. Wu, B.-L. Gu, F. Liu, and W.-H. Duan, Phys. Rev. Lett. **95**, 196803 (2005).

[6] F. B. Mota, V. B. Nascimento, and C. M. C. de Castilho, J. Phys.: Condens. Matter **17**, 4739 (2005).

[7] X. Peng, P. Krüger, and J. Pollmann, Phys. Rev. B **72**, 245320 (2005).

[8] X. Peng, P. Krüger, and J. Pollmann, Phys. Rev. B **76**, 125303 (2007).

[9] M. D'Angelo, H. B. Enriquez, N. Rodriguez, V. Yu. Aristov, P. Soukiassian, A. Tejeda, E. G. Michel, M. Perdido, C. Ottaviani, and P. Perfetti, J. Chem. Phys. **127**, 164716 (2007).

[10] F. Amy, J. Phys. D **40**, 6201 (2007).

[11] H. J. Monkhorst and J. K. Pack, Phys. Rev. B **13**, 5188 (1976).

[12] G. Kresse and J. Hafner, Phys. Rev. B **49**, 14251 (1994); G. Kresse and J. Furthmüller, *ibid.* **54**, 11169 (1996); G. Kresse and D. Joubert, *ibid.* **59**, 1758 (1999).

[13] P. Deák, Th. Frauenheim, and A. Gali, Phys. Rev. B **75**, 153204 (2007).

[14] P. Deák, A. Gali, and B. Aradi, in *Recent Advances in SiC Research*, edited by W. J. Choyke, H. Matsunami, and G. Pensl (Springer, Berlin, 2003) pp. 57–88.

[15] The model itself had been also reoptimized with GGA, following the same procedure as described above for the LDA calculations, but with 25 Å of vacuum above the slab.

[16] M. Elstner, Th. Frauenheim, E. Kaxiras, G. Seifert, and S. Suhai, Phys. Status Solidi B **217**, 357 (2000); H. A. Witek, K. Morokuma, and A. Stradomska, J. Theor. Comput. Chem. **4**, 639 (2005).

[17] G. S. Higashi, Y. J. Chabal, G. W. Trucks, and K. Raghavachari, Appl. Phys. Lett. **56**, 656 (1990).

[18] N. Sieber, T. Stark, Th. Seyller, L. Ley, C. A. Zorman, and M. Mehregany, Appl. Phys. Lett. **80**, 4726 (2002).

[19] Y. J. Chabal and K. Raghavachari, Phys. Rev. Lett. **54**, 1055 (1985).

[20] W. Lu, P. Krüger, and J. Pollmann, Phys. Rev. B **60**, 2495 (1999).

[21] B. Szűcs, A. Gali, Z. Hajnal, P. Deák, and C. G. Van de Walle, Phys. Rev. B **68**, 085202 (2003).

[22] G. Lucovsky, Solid State Commun. **29**, 571 (1979); S. N. Sahu, T. P. Shi, P. W. Ge, J. W. Corbett, A. Hiraki, T. Imura, M. Takashiro, and V. A. Singh, J. Chem. Phys. **77**, 4330 (1982).

[23] P. Deák, M. Heinrich, L. C. Snyder, and J. W. Corbett, Rev. Solid State Sci. **5**, 403 (1991).

[24] D. B. Laks, C. G. Van de Walle, G. F. Neumark, P. E. Blöchl, and S. T. Pantelides, Phys. Rev. B **45**, 10965 (1992).

[25] L. Pizzagalli, A. Catellani, G. Galli, F. Gygi, and A. Baratoff, Phys. Rev. B **60**, R5129 (1999).

[26] W. Lu, W. G. Schmidt, E. L. Briggs, and J. Bernholc, Phys. Rev. Lett. **85**, 4381 (2000).

[27] A. Baldereschi, S. Baroni, and R. Resta, Phys. Rev. Lett. **61**, 734 (1988).

[28] A. Qteish, V. Heine, and R. J. Needs, Phys. Rev. B **45**, 6534 (1992).

[29] P. Soukiassian (private communication).

[30] C. G. Van de Walle and R. A. Street, Phys. Rev. B **51**, 10615 (1995).

[31] J. I. Pascual, J. J. Jackiw, Z. Song, P. S. Weiss, H. Conrad, and H.-P. Rust, Phys. Rev. Lett. **86**, 1050 (2001).

[32] J. Roy, V. Yu. Aristov, C. Radtke, P. Jaffrennou, H. Enriquez, P. Soukiassian, P. Moras, C. Spezzani, C. Crotti, and P. Perfetti, Appl. Phys. Lett. **89**, 042114 (2006).